

Conceptual Designs of 50MW_e and 450MW_e Supercritical CO₂ Turbomachinery Trains for Power Generation from Coal. Part 2: Compressors

Rahul A. Bidkar^(a), Grant Musgrove^(b), Meera Day^(b), Chris D Kulhanek^(b), Tim Allison^(a),
Andrew M Peter^(a), Doug Hofer^(a), Jeff Moore^(b)

(a) General Electric Company, GE Global Research, One Research Circle, Niskayuna, NY 12309 USA
(b) Southwest Research Institute, P.O. Box 28510, Division 18, San Antonio, TX 78228 USA

ABSTRACT

Supercritical CO₂ power cycles could be a more efficient alternative to steam Rankine cycles for power generation from coal. However, CO₂ turbomachinery for this application has not yet been designed. This paper summarizes a clean-sheet conceptual design of the main compressor and recompressor for a 450MW_e reheat cycle. Preliminary stage counts and sizing were selected to optimize specific speed and diameter. These designs were then refined using the meanline prediction code COMPAL. Analysis results show it is possible to package a 2-stage main compressor and 4-stage recompressor at 3600 rpm into a single casing in a back-to-back arrangement and still maintain rotordynamic stability. Predicted component performance maps have been generated for varying inlet volume flow. Turbomachinery design is compared with other CO₂ turbomachinery concepts in open literature. Finally, an overall layout of the single-shaft machine with a dual-flow high-pressure turbine and a dual-flow low-pressure turbine directly coupled with a back-to-back compressor and recompressor is also discussed in this paper.

1. INTRODUCTION

Closed-loop recompression Brayton cycles using supercritical carbon dioxide (sCO₂) as a working fluid have been proposed to replace steam for power generation from pulverized coal [1]. The primary benefit to using sCO₂ as a working fluid in such a cycle is that it can achieve higher thermal cycle efficiency (up to 5 points [1]) at the equivalent turbine inlet conditions of state-of-the-art ultrasupercritical steam plants. This efficiency gain is due to the transfer of thermal energy from coal combustion to the sCO₂ power cycle at a higher average temperature than in a comparable steam cycle. Additional benefits include reduced water consumption, reduced power block size (smaller turbomachinery and condenser due to the higher working fluid density), and better thermodynamic integration with post-combustion CO₂ capture and compression equipment as shown by Moullec [1]. These benefits make sCO₂ turbomachinery an attractive possibility for power generation. In a companion Part-1 paper [2], thermodynamic cycles and turbine layouts for 50 MW_e and 450 MW_e sCO₂ turbines were presented. In this Part-2 paper, the compressor and recompressor layout are described for direct coupling with the 450 MW_e turbine discussed in the Part-1 paper [2]. The turbine layout discussed in the Part-1 paper [2] and the compressor/recompressor layout discussed in this Part-2 paper

together are intended to demonstrate feasibility of a utility-scale power plant with $s\text{CO}_2$ as the working fluid.

Based on a literature review of large-scale compressors, very few single-shaft designs for $s\text{CO}_2$ recompression-cycle compressors have been developed. In a single-shaft layout (see Figure 1), the compressor and the recompressor are housed in a back-to-back arrangement and supported on a single bearing span inside a single casing. This compressor/recompressor train is then directly coupled with the turbine rotor and runs at the same speed as the turbine rotor. There are numerous advantages to this single-shaft architecture. A single-shaft design eliminates end seal leakage from additional machinery casings as well as power losses from additional bearings, gearboxes, and does not require a separate drive motor to start the cycle. However, the single-shaft layout also introduces design constraints and several technological challenges on the compressor design. A single casing for the compressor and recompressor requires the impeller diameters of both the compressor and the recompressor to be similar in size. Furthermore due to rotordynamic concerns, during the preliminary design process, the design is constrained to have a maximum shaft length-to-diameter (L/D) ratio less than 10. This constraint results in limits to the number of stages of both machines. Validity of the L/D constraint during the preliminary design needs to be verified using a rotordynamic stability analysis. Another concern for the preliminary design and allowing a single casing was the arrangement of the stages to mitigate thrust imbalance. As commonly done to balance axial thrust, the main compressor and recompressor were expected to be in a back-to-back arrangement to balance the axial thrust of each stage.

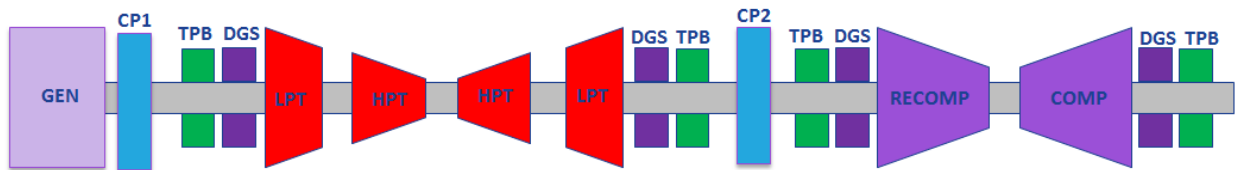


Figure 1 Single-shaft layout showing the turbine rotor coupled with compressor/recompressor, GEN -generator, CP1 - generator-side coupling, TPB - tilt-pad bearing; DGS - dry gas seals, HPT - high-pressure turbine, LPT - low-pressure turbine; CP2 - compressor-side coupling, RECOMP – recompressor, COMP - compressor

This paper presents a conceptual design and a preliminary design for a single-shaft back-to-back compressor/recompressor for a 450 MW_e $s\text{CO}_2$ plant. The conceptual design method (the Baljé chart method [3]) utilizes experience charts for non-dimensional design parameters to establish basic stage geometry and performance. The conceptual design results are then used as inputs for preliminary design using COMPAL [4]; commercially available meanline prediction software for compressor design. These results are presented in Section 2. The rotordynamic analysis for this compressor/recompressor train is presented in Section 3. The compressor/recompressor design from this Part-2 paper and the turbine layouts from the companion Part-1 paper [2] are compared with other designs in open literature in Section 4. Finally, the combined turbine-compressor layout for the $s\text{CO}_2$ power plant is presented in Section 5 along with a summary of the present work in Section 6.

2. COMPRESSOR AND RECOMPRESSOR SIZING FOR a 450 MW_e cycle

Preliminary sizing of the main compressor and recompressor was performed to determine the feasibility of the compressors for the predicted cycle conditions. The operating conditions used for designing the compressor and recompressor are based on the thermodynamic cycle presented in the Part-1 paper [2] and are listed in Table 1¹. The nomenclature used for describing the designs is listed in the Appendix. Two methods were used for sizing the compressors, (a) the Baljé chart method [3], and (b) compressor meanline prediction software, COMPAL [4]. The output of the Baljé method was used as a starting point for the COMPAL design. First, the Baljé method and the sizing based on this method are discussed. This is followed by the compressor and recompressor sizing obtained using COMPAL.

Table 1 Operating conditions for compressor and recompressor design

Parameter	Units	Main Compressor	Recompressor
Inlet Pressure P_1	bara	65.9	67.1
Inlet Temperature T_1	°C	21.5	54.8
η_{target}	-	0.79	0.8
Max speed	rpm	3600	3600

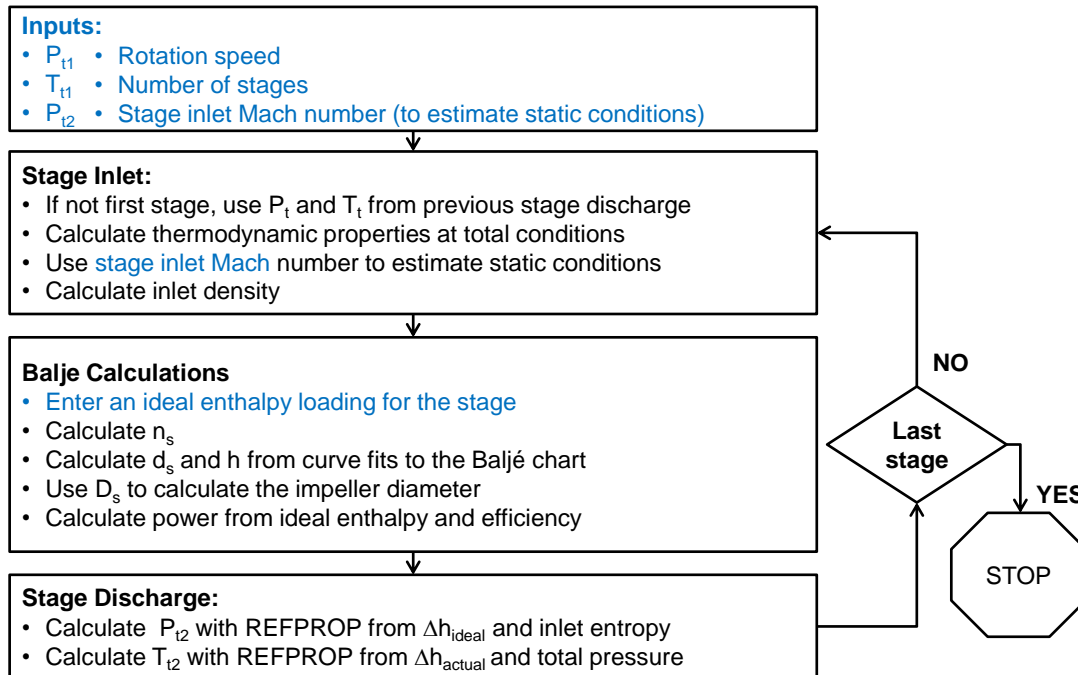


Figure 2: Flowchart of compressor sizing procedure for each stage of a multistage machine.

¹ The conditions listed in Table 1 are the final optimal cycle conditions from the Part-1 paper [2]. The compressor and recompressor design was performed for a non-optimal cycle with slightly different pressures and temperatures. At this preliminary design stage, the compressor and recompressor designs were not expected to change significantly with this slight change in operating conditions.

The goal of the Baljé sizing method [3] was to identify the number of stages necessary to both achieve the cycle efficiency targets as well as obtain a bearing span length-to-diameter (L/D) ratio less than 10. A single shaft layout in a back-to-back configuration as shown in Figure 1 was chosen. The Baljé sizing method [3] was used to determine the efficiency while additional correlations are used to estimate the shaft diameter and aerodynamic stage length. The Baljé method uses non-dimensional compressor sizing parameters of specific speed (n_s) and specific diameter (d_s) to estimate compressor size and efficiency from a commonly-accepted experience chart for compressors. The design process using the Baljé chart method is summarized in Figure 2. Because the Baljé chart is for a single stage compressor, it was applied on a stage-by-stage basis to estimate the sizing of a multi-stage compressor for the design conditions. The diameter of the shaft is approximated as the impeller hub diameter. The impeller hub is sized by assuming an inlet axial Mach number of 0.3 or less and utilizing a correlation for inlet shroud diameter based on radial inflow turbines [5]. The length of the aerodynamic stages is approximated using a correlation from Aungier [6] for the axial length of an impeller. The stage length is estimated to be twice the impeller axial length.

The Baljé sizing method was completed for a range of stage counts on the main compressor and recompressor to find that a two-stage main compressor and a five-stage recompressor are required to meet the compressor efficiency targets set by the cycle. This is shown in Figure 3. Apart from meeting the efficiency targets, the compressor/recompressor train also needed to satisfy the requirement of L/D ratio less than 10. This requirement was driven by the rotordynamic stability requirements. As mentioned earlier, the hub diameter and the axial stage length was calculated for each of the combinations shown in Figure 3 using the inlet Mach number criterion [5] and the Aungier correlation [6]. In order to estimate the overall L/D for the compressor and the recompressor, an estimate for the axial length of various components of the compressor assembly was needed. The compressor assembly typically comprises of bearings, dry gas seals, balance piston drum, inlet and exit sections of the recompressor, the recompressor impellers, the main compressor impellers, and the inlet and exit sections of the main compressor. Using experience-based aspect ratios, the axial lengths of the bearings, balance piston, and dry gas seals were estimated. The axial lengths of the inlet and exit sections that house the inlet and exit plenums were sized such that the flow losses were small. The resulting L/D ratio for all configurations is shown in Figure 4.

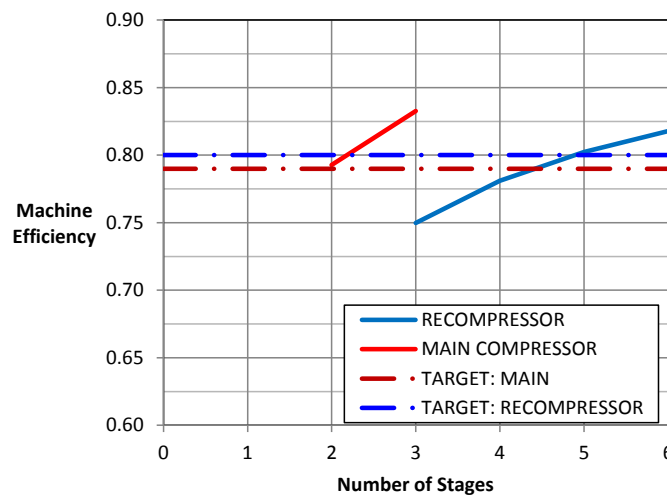


Figure 3. Comparison of 450 MW_e Compressor Efficiency (Baljé Method) to the Cycle Targets for a Range of Stage Counts

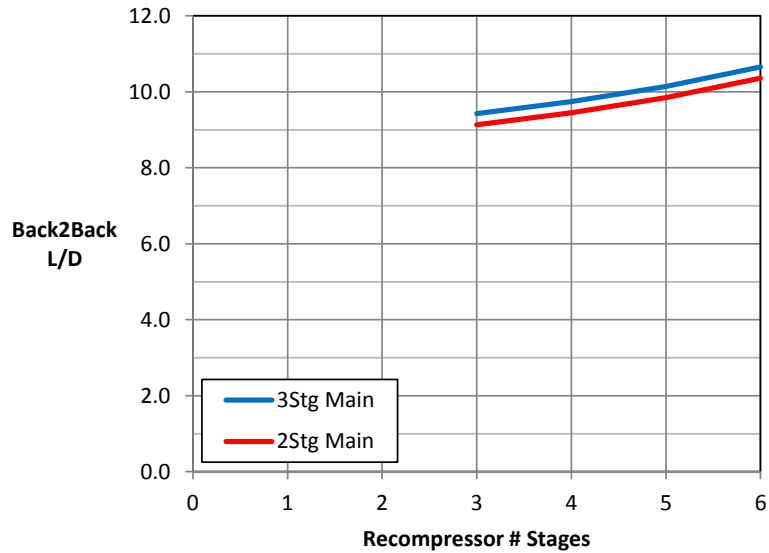


Figure 4 Machine L/D prediction for a Back-to-Back 450 MW_e Machine Configuration (Baljé Method)

The configuration with a two-stage main compressor and a four-stage recompressor was selected. The two-stage main compressor was chosen because it was sufficient to meet the efficiency target while also reducing the L/D ratio. Even though the four-stage recompressor does not meet the efficiency target, the reduction of machine L/D was decided to be more important at this stage for design feasibility than the efficiency target. These results of the Baljé method were used as a starting point for meanline design predictions software, COMPAL [4].

Commercial meanline prediction software, COMPAL [4] by Concepts NREC, was used to generate preliminary flow-path. COMPAL predictions are based on the Euler turbomachinery equation. While the Baljé sizing method uses non-dimensional parameters to estimate compressor efficiency based on design experience, COMPAL utilizes loss models. When combined, these loss models can estimate compressor efficiency based on geometry and operating conditions. Therefore, using COMPAL allows for a more detailed definition of the geometry of the stages and allows for a better estimation of the resulting efficiency.

To generate the COMPAL design, the hub diameter, the impeller axial length and the average impeller tip diameter obtained from the Baljé sizing method were used as inputs to the COMPAL software. The COMPAL result was generated by allowing the software to optimize the discharge impeller width and discharge blade angles. Because of the similar impeller tip diameters, the COMPAL design matches the specific speed and specific diameter values of the Baljé sizing method. Similarly, other compressor parameters like the flow coefficient, polytropic head and efficiency matched well between the Baljé method and COMPAL method. This is shown for the recompressor in Figure 5 and Figure 6. COMPAL-optimized designs, however, do not agree with conventional compressor designs in certain aspects such as impeller axial widths and impeller back-sweep angles. The inputs to COMPAL design software were modified so that the final COMPAL prediction agreed with conventional compressor designs.

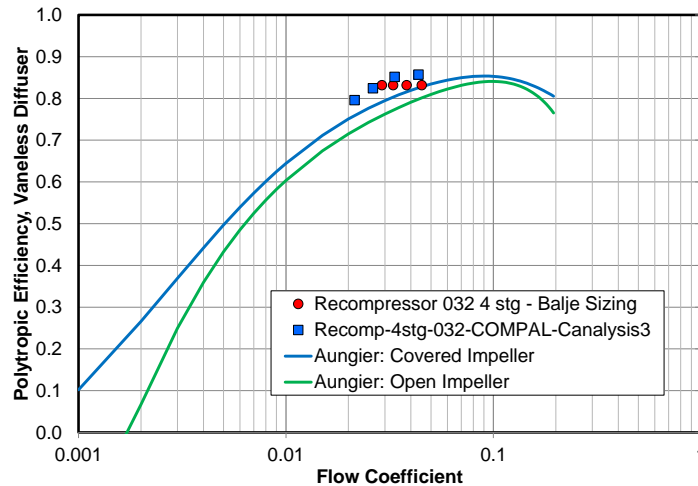


Figure 5 Comparison of Polytropic Efficiency between the COMPAL 450 MW_e Recompressor Design, the Baljé Sizing Method, and Aungier’s Sizing Correlations

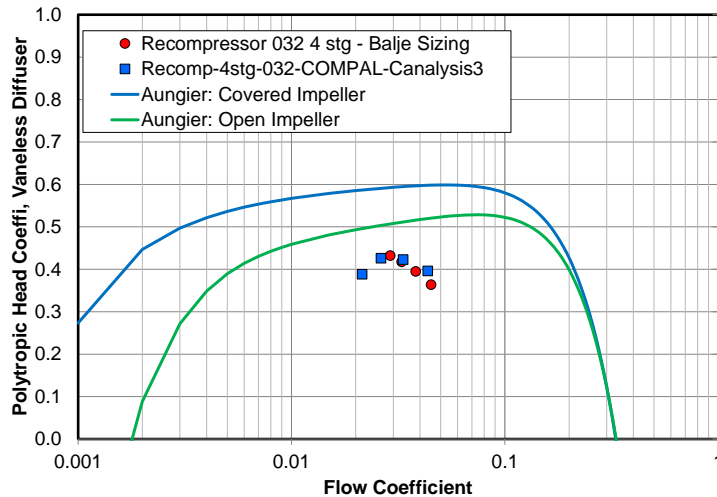


Figure 6 Comparison of Polytropic Head Coefficient between the COMPAL 450 MW_e Recompressor Design, the Baljé Sizing Method, and Aungier’s Sizing Correlations

In summary, the preliminary COMPAL results were found to be close enough to the Baljé sizing method to give confidence in using either method to define a preliminary compressor design. Starting from the initial sizing using the Baljé method, COMPAL can be used to obtain a better definition of stage geometry and a more accurate estimate of compressor efficiency. Additionally, COMPAL can be used to create performance maps of the preliminary compressor design. To generate performance maps, the operation of the recompressor was estimated over a range of flow rate at constant speed. This is shown in Figure 7. The recompressor design was found to have a wide flow range and its efficiency was found to increase for flow rates less than the design point (design point flow rate is about 9 m³/s). The wide flow range for this design is possible because a vaneless diffuser was used. Performance maps such as the ones shown in Figure 7 are very useful for studying off-design performance of the thermodynamic cycle and allow for further refinement of the cycle model.

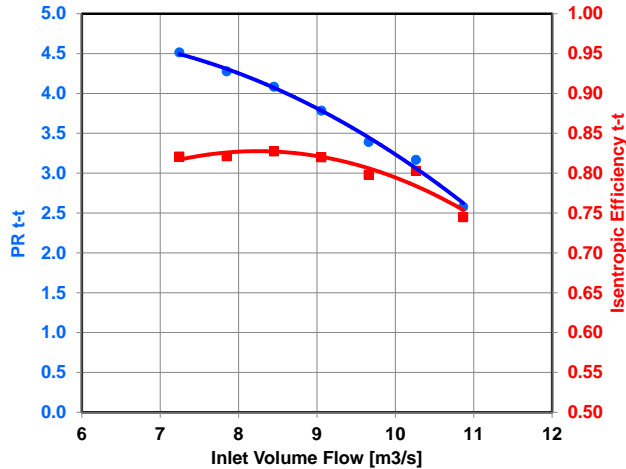


Figure 7 Predicted Performance of the Four-Stage 450 MW_e Recompressor at 3,600 rpm, shown as Total-Total Pressure Ratio and Isentropic Efficiency

The layout of the 4-stage recompressor design using COMPAL is shown in Figure 8. COMPAL does not output an estimate of the radius of curvature between the return channel and the following stage. The curvature of the return channel exit was estimated to be equal to the curvature of the following stage impeller and was included in the L/D calculations.

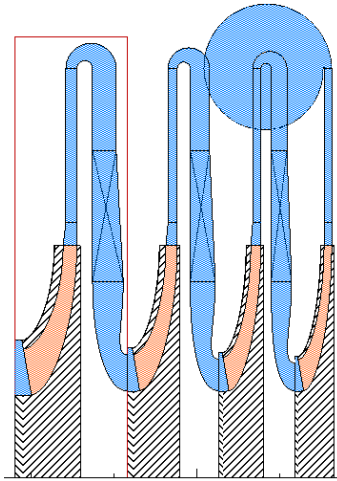


Figure 8 Illustration of Four-Stage 450 MW_e Recompressor Design

Similar to the recompressor, the main compressor was designed using COMPAL with the results of the Baljé sizing method used as inputs. The main compressor inlet pressure was increased slightly from the cycle specifications in order to keep the static thermodynamic properties at the compressor inlet outside of the two-phase region. Similar to the recompressor results (see Figure 5 and Figure 6), the Baljé method and the COMPAL method resulted in similar predictions for polytropic efficiency and polytropic head for the main compressor. Also, similar to the recompressor performance map (see Figure 7), the main compressor performance for non-design-point flow rates was studied. The overall layout of the 2-stage recompressor design using COMPAL is shown in Figure 9.

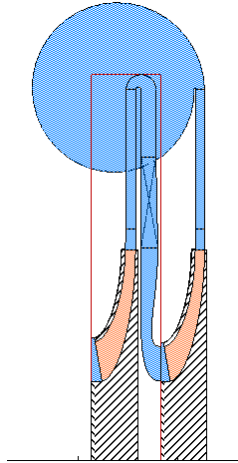


Figure 9 Illustration Two-Stage 450 MW_e Main Compressor Design

Combining the recompressor layout (Figure 8) and the main compressor layout (Figure 9), an overall layout for the back-to-back configuration is shown in Figure 10. Note that the volutes at the exits of the main compressor and the recompressor were designed at an outer radius (unlike Figure 8 and Figure 9) allowing for a shorter span of the back-to-back configuration. The overall L/D ratio for the resulting configuration was about 8.4 instead of L/D of about 11, which would have resulted from the exit volutes located at an inner radius. While the compressor designs are preliminary in nature, they provide a basis for detailed design in future work.

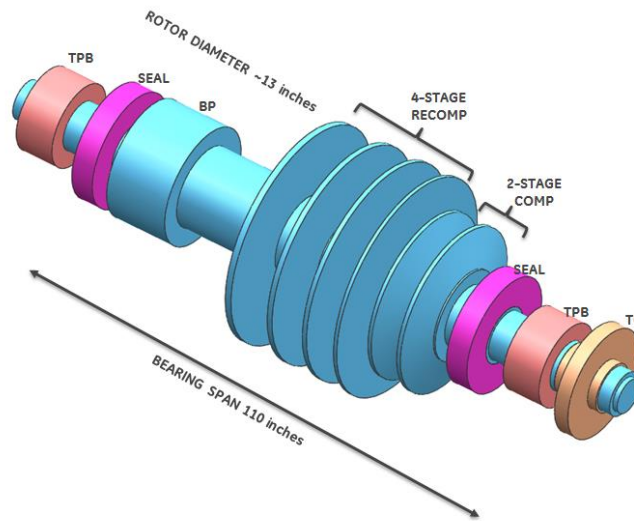


Figure 10 3D layout of the compressor and recompressor, TC - Thrust Collar, TPB - Tilt Pad Bearing, COMP - Main compressor, RECOMP - Recompressor, BP - Balance Piston

3. ROTORDYNAMIC STABILITY ANALYSIS

Rotordynamic stability of the compressor/recompressor was analyzed using the XLTRC2 software developed by Texas A&M University [7]. The solid model of the compressor/recompressor (see Figure 10) was used as a starting point for geometry definition. The rotordynamic model is shown in Figure 11.

Beam elements are used to model the rotor stiffness, and lumped inertia values of the impellers, dry-gas seals and coupling half weights are used to model the mass of various elements. Tilt-pad journal bearings were used in this study with both nominal stiffness and a relatively larger stiffness. Bearing stiffness calculations were performed using THPAD bearing code, which is part of the ROMAC rotordynamic codes.

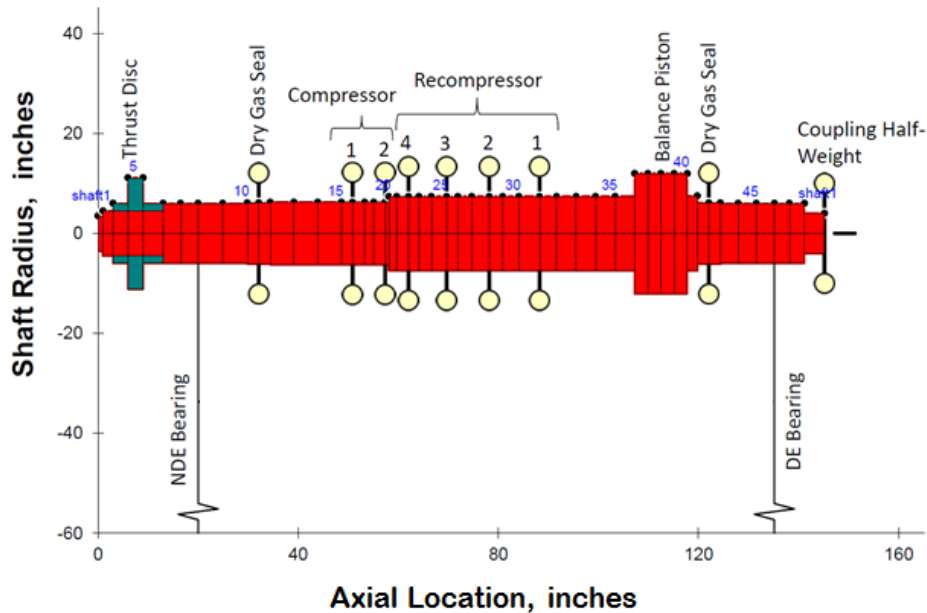


Figure 11 Rotordynamic model for the compressor/recompressor

Two rotor lengths were analyzed to study the effect of length on the rotordynamic stability. The first case involved a nominal-length compressor described above, while the second case involved a rotor with 15% increased length. Overall, this resulted in four combinations resulting from two levels for bearing stiffness and two possible lengths for the rotor. Damping and stiffening effects of labyrinth seals for impeller eye location, labyrinth seals with swirl brakes for the balance piston location and hole pattern seals for the balance piston location were also investigated.

The goal of the rotordynamic analysis was to study the forced unbalance response of rotor and evaluate the stability of the rotor. The first critical speed, based on the imbalance response without seal effects, is predicted to be approximately 2,900 to 3,100 rpm for the nominal rotor (different values represent different bearing stiffness cases), and about 2,400 to 2,500 rpm for the increased length rotor. This is lower than the operating speed of 3600 rpm. Inclusion of the labyrinth seals (for the impeller eye and the balance piston locations) in the model increased the 1st critical speed by approximately 250~300 rpm. Inclusion of the hole-pattern balance piston (HPBP) seal in the model had a significant effect, causing the first mode to further increase to approximately running speed (~3,600 rpm). The nominal rotor length does not meet API separation margin requirements [8] for the 1st critical speed for all cases considered. However, the lengthened rotor with labyrinth seals (for the impeller eye and the balance piston locations) is predicted to meet API separation margins for the 1st critical speed. While the critical speed with the HPBP (lengthened rotor) is placed at running speed, the subject mode is predicted to have amplification factors less than 2.0, and is considered critically damped by API. Thus, the lengthened rotor with nominal bearing stiffness and labyrinth seals is an acceptable rotordynamic configuration.

Furthermore, the lengthened rotor (with either bearing stiffness) and HPBP is yet another acceptable configuration with increased stability compared to the no-HPBP configuration.

Since both acceptable configurations described above need an increased rotor length (and thereby cost), an alternative arrangement with a nominal rotor length was also explored. This configuration had bearings that involved soft mounting the bearing housing and providing a squeeze-film-damper between the bearing housing and ground. This configuration is shown in Figure 12. The soft mounting brings the frequencies of the first two-modes well below the operating speed of 3600 rpm, while keeping the first bending mode (overall third mode) above the operating speed. This change effectively provides the required separation margin. Addition of the HPBP greatly improves the stability. Soft-mounted bearings with squeeze-film damper and HPBP seals is the recommended configuration for the compressor/recompressor train from a rotordynamic standpoint. Furthermore, this configuration also confirms the feasibility of the back-to-back compressor/recompressor concept mounted on a single bearing span and housed in a single casing. In the next section, the compressor/recompressor design from this Part-2 paper and the turbine designs from the companion Part-1 paper [2] are compared with available literature.

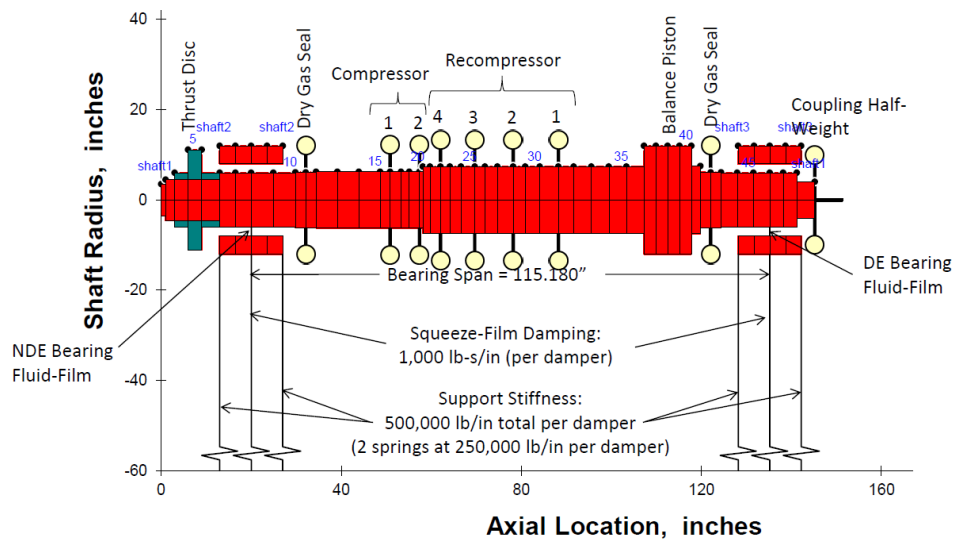


Figure 12 Rotordynamic model for the compressor/recompressor with squeeze-film damper

4. COMPARISON WITH LITERATURE

A literature review was conducted to compare the proposed machinery design with other published designs for utility-scale applications of sCO₂ turbomachinery. Five publications were deemed to be sufficiently similar applications as to merit a deeper review. All information presented for the comparison was taken from publically available sources; therefore, not all fields are populated. A field with information that was unavailable is denoted with a dash. The data, shown in Table 2, show that while there are many applications planned for similar power ranges, there is nothing that exactly aligns

with the conditions discussed here. Nonetheless, the similarities between the previously studied designs and the design presented here are worth discussing.

Operating speeds for turbomachinery above 50 MW are synchronous due to the lack of gearbox technology capable of higher power ranges. The high flow rates for utility-scale cycles correspond to efficient compressor operation at these speeds. No cycles had length-to-diameter ratios significantly larger than 10, which emphasizes the need to keep this parameter close to 10, or preferably lower. The reviewed papers were a mix of axial and radial flow machines, and no studies reviewed here suggested one configuration was superior to the other for this application. Operating conditions for studied cycles are in the same approximate range of this design, suggesting validity of the cycle presented in this paper. Furthermore, from a perspective of non-dimensional specific speed and specific diameter (for the first stage of the main compressor), there is agreement between the present work and the compressor design in the work of Gong et al. [10]. Comparisons with the work of Moulllec [1] and McDowell et al. [12] led to the conclusion that these cycles lie roughly in the same range of the present work. Similar to the main compressor design comparisons, the recompressor design from the present work also agrees well with the recompressor from the work of Gong et al. [10] on a non-dimensional basis.

Table 2 Compressor and Recompressor Geometry, Configuration, and Operating Conditions

Reference/Cycle	Dostal et al. [9]	Gong et al. [10]	Johnson et al. [11]	Moulllec [1]	Mcdowell et al. [12]	Compressor Designs Present Work
Operating Speed [rpm]	3600	3600	-	3600	6000	3600
Length / Diameter [-]	8.6	-	-	6.6	10.2	8.4
Compressor Configuration	Axial	Radial, back to back	Radial, back to back	Axial	Radial, back to back	Radial, back to back
Compressor / Recompressor Power [MW]	- / -	41 / 81	- / -	250/370	131 / 220	65/123
Compressor Inlet / Outlet Pressure [bara]		77/ 200		74/320	77/282	67/ 257
Compressor Inlet / Outlet Temperature [°C]	42 / -	32 / 62	- / -	30/ 104	32 / 72	27 / 60
Compressor Mass Flow [kg/s]	2604	1915	-	5510	2653	2134
Compressor Specific Speed / Diameter (First Stage) [-]	- / -	0.38 / 6.01	- / -	1.06 / 2.95	0.25 / -	0.52 / 5.28
Compressor Efficiency [%]	96	85	-	90	81	83
Recompressor Inlet / Outlet Pressure [bara]	- / -	80 / 208	-	76 / 319	79 / 280	68 / 255
Recompressor Inlet / Outlet Temperature [°C]	- / -	73 / 164	- / -	95/ 275	77 / 205	65/ 198

Recompressor Mass Flow [kg/s]	1146	1331	-	3240	1398	1282
Recompressor Specific Speed / Diameter (First Stage) [-]	- / -	0.62/ 5.13	- / -	1.70/ 2.10	0.08/ -	0.66 / 4.46
Recompressor Efficiency [%]	94.8	89.8	-	90.0	79.9	80.1

Unfortunately, significantly fewer data were available in literature for the different turbine designs. A comparison with available data is shown in Table 3. The turbines often featured a double flow configuration, like the 450 MW_e turbines [2]. As with the compressors studied, operating conditions are in a similar range to the cycles studied here.

Table 3. Turbine Geometry, Configuration, and Operating Conditions

Reference/Cycle	Dostal et al. [9]	Gong et al. [10]	Johnson et al. [11]	Moullec [1]	Mcdowell et al. [12]	50 MW_e turbine present work [2]	450 MW_e turbine present work [2]
Speed [rpm]	3600	3600	-	3600	6000	9500	3600
Turbine configuration	-	-	Double flow	-	Double flow	Single flow	Double Flow
Turbine Power [MW]			1000	1677	220	14	360
Turbine inlet / outlet pressure [bara]	- / -	- / -	- / -	310.7 / 81.5	275.8 / 81	250.6 / 61.6	250.6 / 131.8
Turbine inlet / outlet temperature [°C]	- / -	- / -	- / -	620/565	704/543	700/ 518	700 / 612
Turbine mass flow [kg/s]	3750	-	-	8750	1150	343	3413
Turbine efficiency	92.9	-	-	93	90.1	90.3	90.6

5. OVERALL LAYOUT OF TURBINE-COMPRESSOR DRIVE

A single shaft, single-casing layout of a dual-flow high-pressure turbine and a dual-flow low-pressure turbine was shown in the companion Part-1 paper [2]. Similarly, the back-to-back compressor-recompressor layout housed in a single casing was shown in this Part-2 paper in Figure 10. The overall coupled layout for the turbine and the compressor trains was schematically shown in Figure 1. Figure 13 shows a solid model representation of the coupled turbine-compressor layout as a concept for a utility-scale sCO₂ power plant.

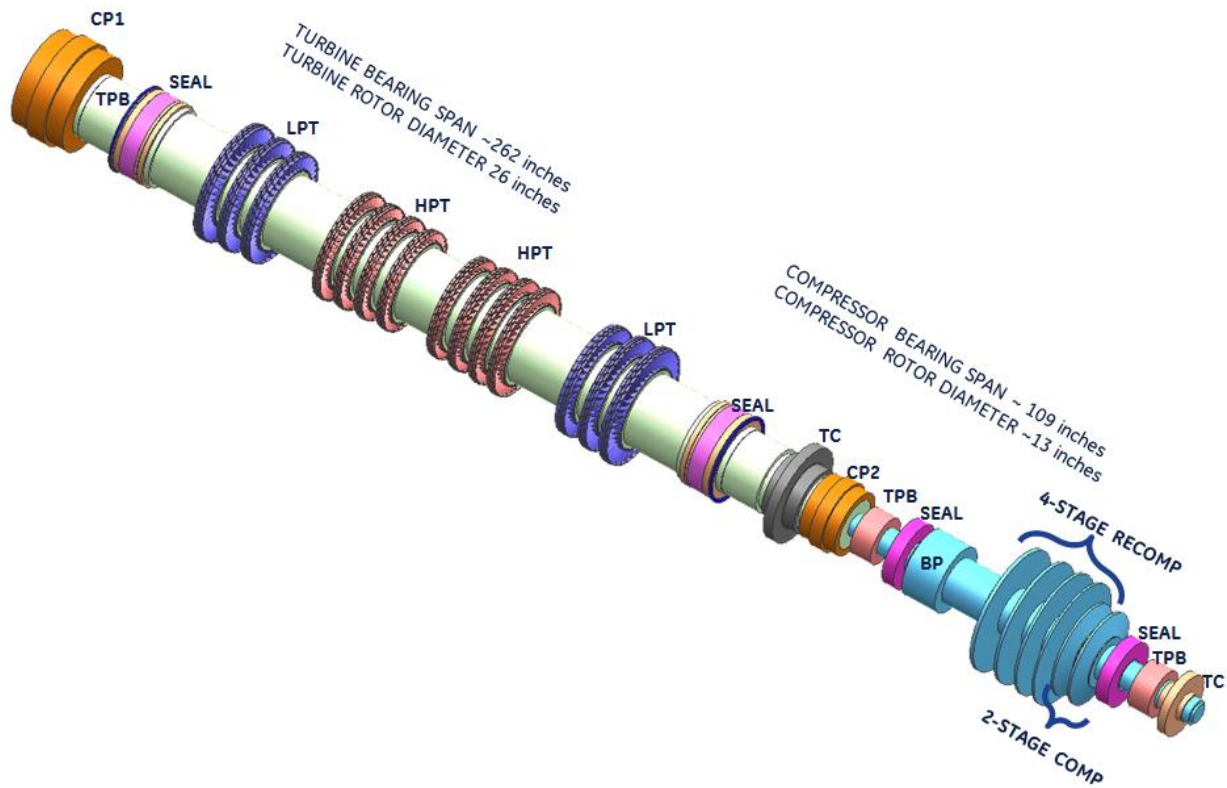


Figure 13 Overall 3D layout of the 450MW_e coupled turbine and compressor train, CP1- generator-side coupling, TPB - tilt pad bearing, LPT - low pressure turbine, HPT - high pressure turbine, TC - thrust collar, CP2 - compressor-side coupling, BP - balance piston, RECOMP – recompressor, COMP – main compressor

6. SUMMARY AND CONCLUSIONS

This paper presented a preliminary design for the compressor and recompressor for a utility-scale sCO₂ power plant. The centrifugal compressors were sized using the Baljé chart method and the design was further refined using COMPAL. A back-to-back configuration based on a 2-stage main compressor and 4-stage recompressor resulted from trade-off studies involving optimizing the aerodynamic performance and the rotordynamic stability of the compressors. The concept designs met the target efficiency requirements set by the thermodynamic cycle and enabled a reheat recompression sCO₂ power cycle with an overall cycle efficiency of 51.9%. Future work could utilize the compressor maps generated in this study to explore the off-design operation and control of such a fixed-speed turbomachinery train.

ACKNOWLEDGEMENT

This material is based upon work supported by the U.S. Department of Energy under Award Number DE-FE0024007. The authors want to thank Dr. Seth Lawson and Richard Dennis at U.S. Dept. of Energy – National Energy Technology Laboratory for his support and guidance during this program.

DISCLAIMER

This paper was prepared as an account of work sponsored by an agency of the United States Government. Neither the United States Government nor any agency thereof, nor any of their employees, makes any warranty, express or implied, or assumes any legal liability or responsibility for

the accuracy, completeness, or usefulness of any information, apparatus, product, or process disclosed, or represents that its use would not infringe privately owned rights. Reference herein to any specific commercial product, process, or service by trade name, trademark, manufacturer, or otherwise does not necessarily constitute or imply its endorsement, recommendation, or favoring by the United States Government or any agency thereof. The views and opinions of authors expressed herein do not necessarily state or reflect those of the United States Government or any agency thereof.

REFERENCES

- [1] Y. L. Moullec, "Conceptual study of a high efficiency coal-fired power plant with CO₂ capture using a supercritical CO₂ Brayton cycle," vol. 49, pp. 32-46, 2013.
- [2] R. A. Bidkar, A. Mann, R. Singh, E. Sevincer, S. Cich, M. Day, C. D. Kulhanek, A. M. Thatte, A. M. Peter, D. Hofer and J. Moore, "Conceptual Designs of 50 MWe and 450 MWe Supercritical CO₂ Turbomachinery Trains for Power Generation from Coal, Part 1: Cycle and Turbine," San Antonio, TX, 2016.
- [3] O. E. Balje, *Turbomachines: A Guide to Design Selection and Theory*, New York, NY: John Wiley & Sons, 1981.
- [4] Concepts NREC, 2015. [Online]. Available: <http://www.conceptsnrec.com/>.
- [5] "Turbine Design and Application," NASA, Washington, DC, 1994.
- [6] R. H. Aungier, *Centrifugal Compressors: A Strategy for Aerodynamic Design and Analysis*, ASME Press, 2000.
- [7] The Turbomachinery Laboratory, Texas A&M University, 2014. [Online]. Available: <http://turbolab.tamu.edu>.
- [8] API Standard 617, *Axial and Centrifugal Compressors and Expander-Compressors for Petroleum, Chemical and Gas Industry Services*, Washington, D.C.: American Petroleum Institute, 2002.
- [9] V. Dostal, M. J. Driscoll and P. Hejzlar, "A supercritical carbon dioxide cycle for next generation nuclear reactors," 2004.
- [10] Y. Gong, N. A. Carstens, D. M. J and M. I. A, "Analysis of radial compressor options for supercritical CO₂ power conversion cycles," 2006.
- [11] G. A. Johnson, M. W. McDowell, G. M. O'Connor, C. G. Sonawane and G. Subbaraman, "Supercritical CO₂ cycle development at Pratt & Whitney Rocketdyne," Copenhagen, Denmark, 2012.
- [12] M. McDowell, A. Eastland, M. Huang and C. Swingler, *Advanced Turbomachinery for sCO₂ Power Cycles*, Atlanta, GA: University Turbine Systems Research Workshop, 2015.

APPENDIX: NOMENCLATURE USED FOR COMPRESSOR/RECOMPRESSOR DESIGN

D_2	Impeller tip diameter
d_s	Specific diameter, $d_s = D_2 * Dh_{ideal}^{0.25} / Q^{0.5}$ [-]
Dh	Enthalpy change [J/kg]
F	Flow coefficient, $f = Q_1 / (\pi N D_2^3 / 30)$ [-]
N	Compressor rotation speed [rpm]
n_s	Specific speed, $n_s = N * Q^{0.5} / Dh_{ideal}^{0.75}$ [-]
P	Pressure

Q	Volumetric flow [m^3/s]
T	Temperature
W	Mass flow rate [kg/s]

Subscripts

1	Impeller inlet
2	Impeller exit
h	Hub
s	Shroud
t	Total conditions
θ	Tangential velocity component
z	Axial length

Greek

η	
θ	Tangential component of velocity
ρ	Density

AUTHOR BIOGRAPHIES



Dr. Rahul Bidkar is a Mechanical Engineer at GE Global Research Center in Niskayuna, NY. He received his Ph.D. in Mechanical Engineering from Purdue University. At GE, Rahul has led development of several film-riding turbomachinery seals with applications to aircraft engines, gas turbines, steam turbines and supercritical CO₂ turbines along with coatings development work for fluid drag reduction. He has authored over 10 technical papers, 14 patent applications with 4 granted patents.



Grant Musgrove is Senior Research Engineer in the Machinery Program at Southwest Research Institute. He currently conducts applied research for turbomachinery applications in oil and gas, power generation, and propulsion applications. Mr. Musgrove has experience with the aerodynamic design of radial machinery for both large-scale power generation and small-scale propulsion. His active research areas are turbomachinery design, wet gas compression, and supercritical CO₂. Mr. Musgrove earned his B.S. and M.S. in Mechanical Engineering from Oklahoma State University and from The Pennsylvania State University.

University and from The Pennsylvania State University.



Meera Day is an Engineer in the Rotating Machinery Dynamics Section at Southwest Research Institute in San Antonio, TX. While at SwRI, her research has included instrumentation, performance testing, control systems, and rotordynamics analysis intended for applications such as turboexpanders, centrifugal compressors, and utility scale cycles. She has Bachelor of Science degrees in Mechanical Engineering and Mathematics from Southern Methodist University.



Dr. Tim Allison is the manager of the Rotating Machinery Dynamics Section at Southwest Research Institute in San Antonio, TX. His research at SwRI includes finite element analysis, modal testing, instrumentation, and performance testing for applications including high-pressure turbomachinery, centrifugal compressors, gas turbines, reciprocating compressor valves, and test rigs for rotordynamics, blade dynamics, and aerodynamic performance. He holds a Ph.D. in Mechanical Engineering from Virginia Polytechnic Institute and State University.



Dr. Peter is a Principal Engineer at GE Global Research Center in Niskayuna, NY. He received his Ph.D. in Aeronautical Engineering from the University of Washington. While at GE, he has worked on gas turbines, fuel cells, boiling water nuclear reactors, concentrating solar power, and supercritical CO₂ turbomachinery. He has also been a product line leader for GE's Integrated Solar Combined Cycle system.



Dr. Douglas Hofer is a Senior Principal Engineer at the GE Global Research Center in Niskayuna NY. His research interests are in the areas of turbomachinery aero-thermal fluid dynamics, advanced expander and compressor technologies, two-phase flows, non-ideal gasses, and transonic and supersonic flows. He has deep experience in the steam turbine industry both in turbomachinery design and cycle analysis and innovation.



Dr. Jeffrey Moore is an Institute Engineer in the Machinery Section at Southwest Research Institute in San Antonio, TX. He holds a B.S., M.S., and Ph.D. in Mechanical Engineering from Texas A&M University. His professional experience over the last 25 years includes engineering and management responsibilities related to centrifugal compressors and gas turbines at Solar Turbines Inc. in San Diego, CA, Dresser-Rand in Olean, NY, and Southwest Research Institute in San Antonio, TX. His interests include advanced power cycles and

compression methods, rotordynamics, seals and bearings, computational fluid dynamics, finite element analysis, machine design, controls and aerodynamics. He has authored over 30 technical papers related to turbomachinery and has two patents issued and two pending. Dr. Moore is the Vanguard Chair of the Structures and Dynamics Committee and has held the position of Oil and Gas Committee Chair for IGTI Turbo Expo. He is also the Associate Editor for the Journal of Tribology and a member of the IGTI SCO2 Committee, Turbomachinery Symposium Advisory Committee, the IFToMM International Rotordynamics Conference Committee, and the API 616 and 684 Task Forces.